

Accepted Manuscript

Synthesis and spectroscopic properties of a copper(II) binuclear complex of a novel tetradentate asymmetrical Schiff base ligand and its DFT study

Iman Rajaei, Seyed Nezamoddin Mirsattari

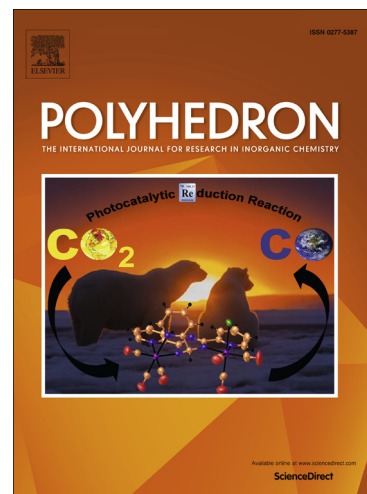
PII: S0277-5387(15)00600-2
DOI: <http://dx.doi.org/10.1016/j.poly.2015.10.019>
Reference: POLY 11604

To appear in: *Polyhedron*

Received Date: 2 June 2015
Accepted Date: 6 October 2015

Please cite this article as: I. Rajaei, S.N. Mirsattari, Synthesis and spectroscopic properties of a copper(II) binuclear complex of a novel tetradentate asymmetrical Schiff base ligand and its DFT study, *Polyhedron* (2015), doi: <http://dx.doi.org/10.1016/j.poly.2015.10.019>

This is a PDF file of an unedited manuscript that has been accepted for publication. As a service to our customers we are providing this early version of the manuscript. The manuscript will undergo copyediting, typesetting, and review of the resulting proof before it is published in its final form. Please note that during the production process errors may be discovered which could affect the content, and all legal disclaimers that apply to the journal pertain.



Synthesis and spectroscopic properties of a copper(II) binuclear complex of a novel tetradentate asymmetrical Schiff base ligand and its DFT study

Iman Rajaei^a, Seyed Nezamoddin Mirsattari^{a,b*}

^aDepartment of Chemistry, Shahreza Branch, Islamic Azad University, P.O Box 311-86145, Shahreza, Isfahan, Iran

^bRazi Chemistry Research Center (RCRC), Shahreza Branch, Islamic Azad University, Isfahan, Iran

Abstract

A new asymmetrical Schiff base ligand, N,N'-(salicylidene)-5-bromo-2-hydroxybenzaldehyde-*p*-phenylenediamine (SBHBP), and its binuclear Cu(II) complex have been synthesized. The molecular structures and spectroscopic properties of the ligand and its complex were experimentally characterized by elemental analysis, FT-IR, NMR and UV–Vis spectroscopic techniques and computationally by the density functional theory (DFT) method. The molecular geometry and vibrational frequencies of the SBHBP ligand in the ground state have been calculated using the B3LYP/6-31G(d,p) and 6-31++G(d,p) basis sets. A potential surface scan study was carried out and the most stable geometry of the SBHBP ligand was confirmed. The calculated results show that the optimized geometry can well reproduce the structural parameters, and the theoretical vibrational frequencies are in good agreement with the experimental values. On calculation of the electronic absorption spectra, TD-DFT calculations were carried out in both the gas and solution phases. The energetic behavior of the SBHBP ligand has been examined in solvent media using the B3LYP method with the 6-31G(d,p) and 6-31++G(d,p) basis sets by applying the Onsager method and polarizable continuum model (PCM). Additionally, Mulliken and NBO atomic charges, NMR analysis, molecular electrostatic potential (MEP) and frontier molecular orbitals (FMO) analysis of the SBHBP ligand were investigated using theoretical calculations.

Keywords: Asymmetric; Schiff base; Binuclear complex; DFT; MEP; Tautomer

1. Introduction

Compounds with the structure XC=NY are known as Schiff bases, and these compounds are usually synthesized by the condensation of primary amines and active carbonyl groups. Schiff bases are used as starting materials in the synthesis of important drugs such as antibiotic, antiallergic, antitumor and antifungal drugs because of their biological activities [1,2]. They have also been widely used as ligands in the field of coordination chemistry [3,4]. Transition metal Schiff base complexes have many applications in industrial [5,6], pharmaceutical [7,8], anti-microbial, antifouling, antiviral agent, antioxidant [9,10] and chemical fields [11,12].

Schiff bases with two imine groups in an aromatic ring can be synthesized by the condensation of diamines with aldehydes or ketones [13,14], or condensation of dialdehydes or diketones with amines [15,16], but a stable compound involving both $-\text{NH}_2$ and $-\text{CHO}$ groups in an aromatic ring cannot be synthesized since these groups react with each other. Therefore, Schiff bases including two asymmetric imino groups attached to the same aromatic ring ($\sim\text{N=HC-Ar-N=CH}\sim$) cannot be synthesized directly. Thus, asymmetric diimines of these types have not been investigated yet, while much literature concerning symmetrical diimines has been published. Herein, we report the synthesis and characterization of a new asymmetric diimine Schiff base *N,N'*-(salicylidene)-5-bromo-2-hydroxybenzaldehyde-*p*-phenylenediamine (SBHBP) and its Cu(II) complex. Also, geometry optimizations and theoretical assignment of the IR, UV-Vis and NMR spectra of the ligand have been performed using the DFT method, which is widely used as a remarkable method in many areas of computational chemistry, such as kinetics and mechanism studies, spectroscopic assignments and thermodynamic parameters [17-19]. In addition the molecular structure, frontier molecular orbital energies, molecular electrostatic potential, and natural bond orbital (NBO) were investigated. These calculations are valuable for providing insight into the molecular properties of Schiff base compounds.

2. Experimental section

2.1. Materials and measurements

All of the chemicals and reagents were purchased from Merck chemical company and used without further purification. The NMR spectrum was recorded on a Bruker Avance 400 MHz spectrometer using d_6 -DMSO as the solvent. FT-IR (KBr pellet, $400\text{-}4000\text{cm}^{-1}$) spectra were taken with a Perkin Elmer 65 FT/IR-4000 spectrometer. The electronic spectra were recorded on a T70 UV/Vis spectrophotometer PG instruments Ltd. Microanalyses (C, H and N) of the ligand and its complex were carried out on a Perkin-Elmer 240C elemental analyzer. An analyst 300 Perkin Elmer atomic adsorption spectrometer was used for the determination of

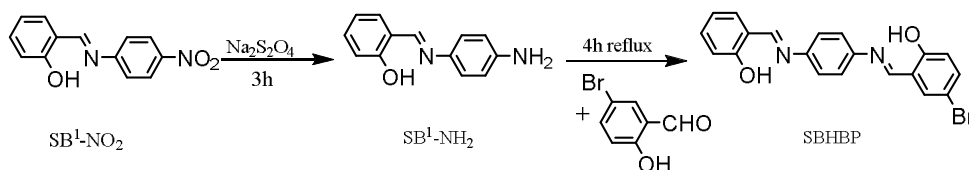
the Cu(II) concentration. Melting points were determined on a Gallen kamp melting point apparatus.

2.2. Synthesis of starting Schiff base ligand (SB¹-NO₂)

The starting Schiff base ligand 2-[[[(4-nitrophenyl)imino]methyl]phenol (SB¹-NO₂) was prepared by refluxing a mixture of a solution containing 4-nitro aniline (1.0 g, 7.24 mmol) in 60 ml ethanol and a solution containing 2-hydroxybenzaldehyde (0.88g, 7.24 mmol) in ethanol (60 ml). The reaction mixture was stirred for 2 h under reflux and allowed to cool. Yield: 90% (dark orange; Elemental Anal. Calc. for C₁₃H₁₀N₂O₃ (242.23 g/mol): C, 64.46; H, 4.16; N, 11.56. Found: C, 63.85; H, 4.43; N, 12.15 %. FTIR (cm⁻¹): ν(O-H) 3437.84; ν(C=N) 1612; ν(NO₂) 1564.03.

2.2.1. Synthesis of the asymmetric diimine

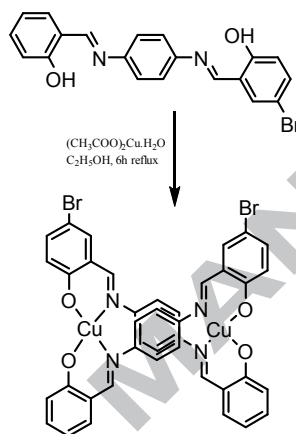
The asymmetric Schiff base was prepared as shown in Scheme 1. The SBHBP ligand was prepared with a two-step method. 1.0 mmol of the starting Schiff base (0.24 g for SB¹-NO₂) was dissolved in an ethanol:water, 1:1 mixture (60 ml) at 70 °C. 5.0 mmol (0.87 g) of solid sodium dithionite was slowly added to the solution in small portions over 1 h and stirred for 2 h at 50 °C for completion of the reducing process. Consequently, the amino derivative of the starting Schiff base (SB¹-NH₂) was formed in the solution. 1.14 mmol of the appropriate aldehyde in 10 ml ethanol was added to this solution dropwise over a period of 1 h with stirring, and the resulting solution was refluxed for 4 h at 60 °C. The yellow precipitate that formed was removed by filtration. Slow evaporation of the mother solution yielded a yellow-white precipitate. Yield: 50.4%. M.p.: 295 °C. Analytical data, UV-Vis and the main IR bands of the SBHBP ligand are summarized in Table 1.



Scheme 1. Synthetic route to the asymmetric Schiff base ligand (SBHBP).

2.2.2. Synthesis of the Cu(II) complex

Copper(II) acetate monohydrate (0.05 g, 0.25 mmol) in EtOH (15 ml) was added, with stirring, to an ethanolic solution (35 ml) of the asymmetric Schiff base ligand (0.10 g, 0.25mmol) and refluxed for 6 h. After removing the solvent, the product was separated, washed with ethanol and dried in vacuum. The probable structure of the complex is shown in Scheme 2. Color: dark green. Yield: 45%. M.p.: 368 °C. Anal. Calc. for $C_{40}H_{26}Br_2Cu_2N_4O_4$ (913.56 g/mol): C, 52.59; H, 2.87; N, 6.13; Cu, 13.91. Found: C, 52.75; H, 2.79; N, 6.10; Cu, 13.15 %. IR (cm^{-1}): $\nu(O-H)$ 3415.3; $\nu(C=N)$ 1608.8. A summary of these results are contained in Table 1.



Scheme 2. Synthetic route to the binuclear Cu(II) complex

2.3. Computational details

The first task for the computational work was to determine the optimized geometry of the asymmetrical ligand. The hybrid B3LYP [20,21] method based on Becke's three parameter functional of DFT and 6-31G(d,p) and 6-31++G(d,p) basis sets level were chosen. All calculations were performed using the Gaussian 09 package program with a molecular visualization program [22,23]. The absence of imaginary frequency modes for the optimised structure of the ligand at the DFT levels confirms a true minimum on the potential energy surface. The most widely used technique for calculating NMR shielding tensors is the GIAO (Gauge Including Atomic Orbital) method [24,25]. This method was used for calculating 1H NMR chemical shifts at the B3LYP level with the 6-31G(d,p) and 6-31++G(d,p) basis sets. In order to evaluate the energetic and atomic charge behavior of the ligand in solvent media, we carried out theoretical calculations in five kinds of solvent ($\epsilon = 78.3553$ - water; $\epsilon = 32.613$ methanol; $\epsilon = 24.852$ - ethanol; $\epsilon = 10.125$ - dichloroethane; $\epsilon = 4.7113$ - chloroform). The

methodologies used in this investigation were centered on two solvation methods: Onsager's reaction field theory [26] of electrostatic solvation and the polarized continuum model (PCM) [27]. The molecular electrostatic potential (MEP) of the optimized structure and the representation of the HOMO, LUMO energy distributions and HOMO–LUMO energy gap [28] density calculations were done at the same level of theory and plotted using the Gauss view program. The B3LYP method has also been used to calculate the dipole moment μ (Debye) and the atomic charges by natural bond orbital (NBO) analysis.

3. Results and discussion

Condensation of aromatic dialdehydes with primary amines or aromatic diamines with aldehydes give symmetrical diimines, $N=C-Ar-C=N$ and $C=N-Ar-N=C$, respectively. Herein, the $C=N-Ar-N=C'$ asymmetric diimine SBHBP was prepared and characterized by elemental analysis, UV-Vis, IR and NMR spectroscopy. Elemental analyses (Table 1) are in agreement with the chemical formula of the compound. The synthesized asymmetric ligand has been used to prepare a binuclear copper(II) complex in the present study. The microanalytical (C, H, N and Cu), IR and UV-Vis data, as collected in Table 1, correspond to the expected composition of this complex.

Table 1. Analytical and selected spectral data of the asymmetric Schiff base ligand and its Cu(II) complex.

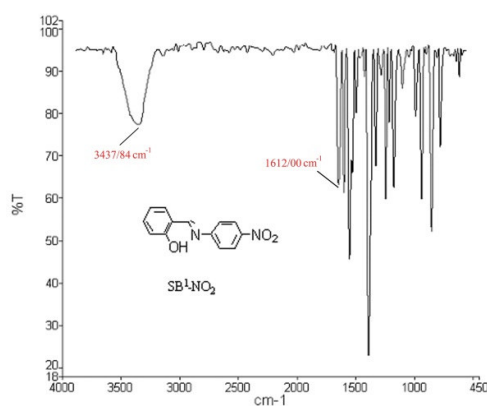
Compound	Found (Calcd)%				λ_{max} (nm)	$\nu(O-H)$ (cm^{-1})	$\nu(C=N)$ (cm^{-1})
	C	H	N	Cu			
SBHBP	60.42(60.78)	3.54(3.83)	7.00(7.09)	—	381,277,244	3438.8	1614.03
$[Cu_2(SBHBP)_2]$	52.75(52.59)	2.79(2.87)	6.10(6.13)	13.15(13.91)	660,387,262,211	—	1608.8

3.1.1. FT-IR study

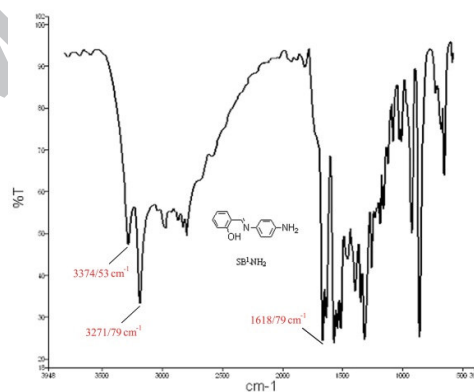
The starting Schiff base (SB^1-NO_2) shows a strong band at 3437.84 cm^{-1} (Fig. 1 (a)) assigned to the (O-H...N) intramolecular hydrogen bonding due to the phenolic OH group of the phenol-imine form [29]. The observation of a sharp and strong band at 1612 cm^{-1} can be assigned to the stretching band of the (C=N) Schiff base imino group. The spectrum of SB^1-NH_2 (Fig. 1 (b)) contains some characteristic bands of the stretching vibrations of the NH_2 and C=N groups. The

IR spectrum of $\text{SB}^1\text{-NH}_2$ shows two bands at 3374.53 and 3271.79 cm^{-1} due to N-H stretching vibrations. These observations show that $\text{SB}^1\text{-NO}_2$ was reduced into the amino derivative ($\text{SB}^1\text{-NH}_2$). The strong band at 1618.79 cm^{-1} corresponds to the stretching vibrations of the C=N bond. The IR spectrum of the asymmetric Schiff base ligand (SBHBP) shows a strong band at 3438.80 cm^{-1} which is assigned to the $\nu(\text{O-H})$ stretching vibration (Fig. 1 (c)). In addition the C=N stretching vibration was observed at 1614.03 cm^{-1} .

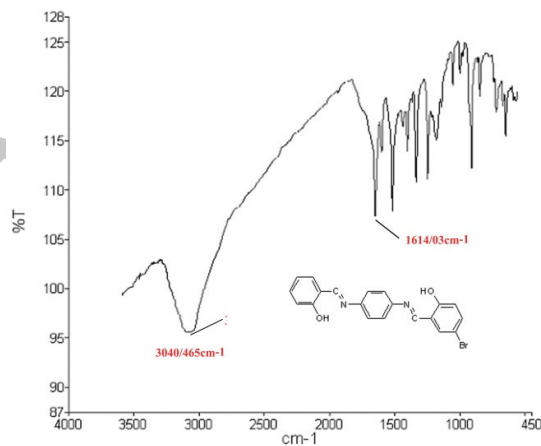
The IR spectrum of the complex was analyzed in comparison with that of the free ligand SBHBP (Fig. 1 (d)). A strong band observed in the spectrum of the complex at 1608.8cm^{-1} is attributable to the azomethine groups. The shift of this band to a lower wavenumber, in comparison to the free ligand, indicates coordination of the azomethine nitrogen atom to the copper(II) ion [30]. Furthermore, the OH stretching band of the phenolic hydroxyl groups of the free ligand disappears in the IR spectrum of the complex, supporting the deprotonation of the phenolic hydroxyl groups of the ligand after complexation.



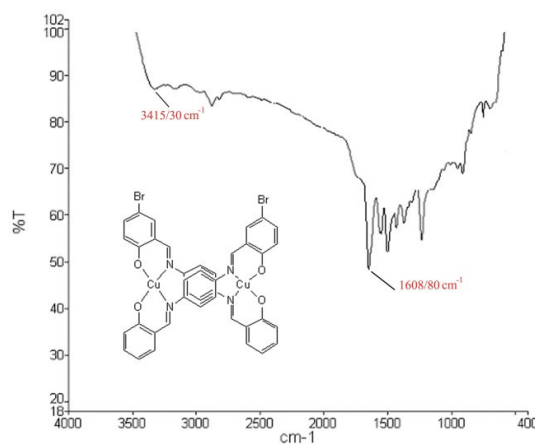
(a)



(b)



(c)



(d)

Fig. 1. Experimental IR spectra of (a) $\text{SB}^1\text{-NO}_2$, (b) $\text{SB}^1\text{-NH}_2$, (c) SBHBP and (d) the $[\text{Cu}_2(\text{SBHBP})_2]$ complex

3.1.2. NMR spectral studies of the ligand

Fig. 2 shows the ^1H NMR spectrum of the Schiff base ligand (SBHBP) in DMSO-d_6 . Experimentally, nine peaks were observed. The synthesis of the SBHBP ligand as a new asymmetric Schiff base was confirmed by the exhibition of three different signals in the range δ 9.00-9.04 ppm, attributed to the asymmetric imines due to different chemical environments. The ^1H NMR spectrum of the SBHBP ligand also exhibits an $\text{OH}_{\text{phenolic}}$ proton resonance at δ 13.05 ppm. The broadening of these absorption peaks may occur due to the involvement of the protons in intra- and intermolecular hydrogen bonding interactions [31]. The multiplets in the δ 6.96-7.90 ppm range can be assignable to the protons of the aromatic rings in the ligand.

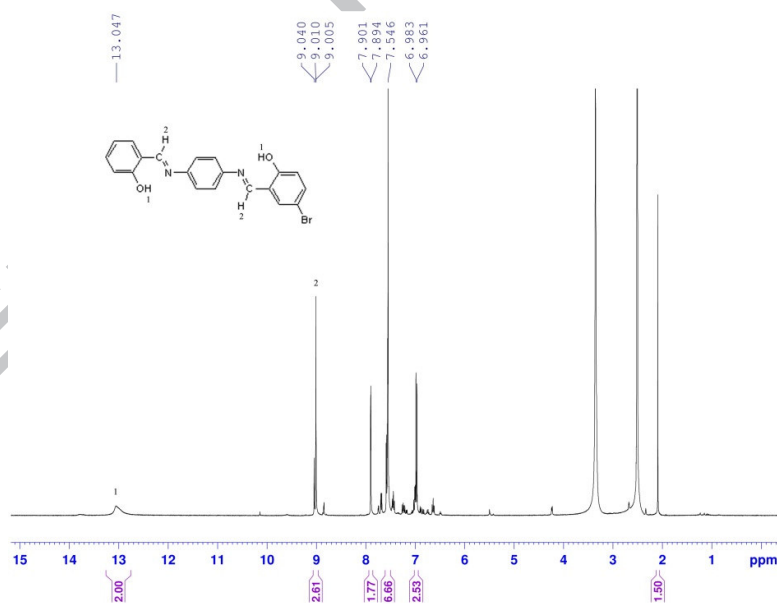


Fig. 2. Experimental ^1H NMR spectrum of the SBHBP ligand

3.1.3. Electronic spectra

The UV-Visible spectrum of the free ligand consists of three strong, sharp discernible bands at around 244, 277 and 381 nm, and these absorptions are in consistent with $\pi-\pi^*$ and $n-\pi^*$ transitions [32,33]. These observations show a blue shift in the first and second absorption bands in the complex, indicating involvement of the azomethine nitrogen and phenolic oxygen atoms in the coordination. Further, the electronic spectrum of the copper complex shows a sharp charge transfer band at around 387 nm and a d-d transition band in the range 660 nm, Fig. 3 (b), the later one is broadened due to the overlap of the d-d transitions with the charge transfer transitions.

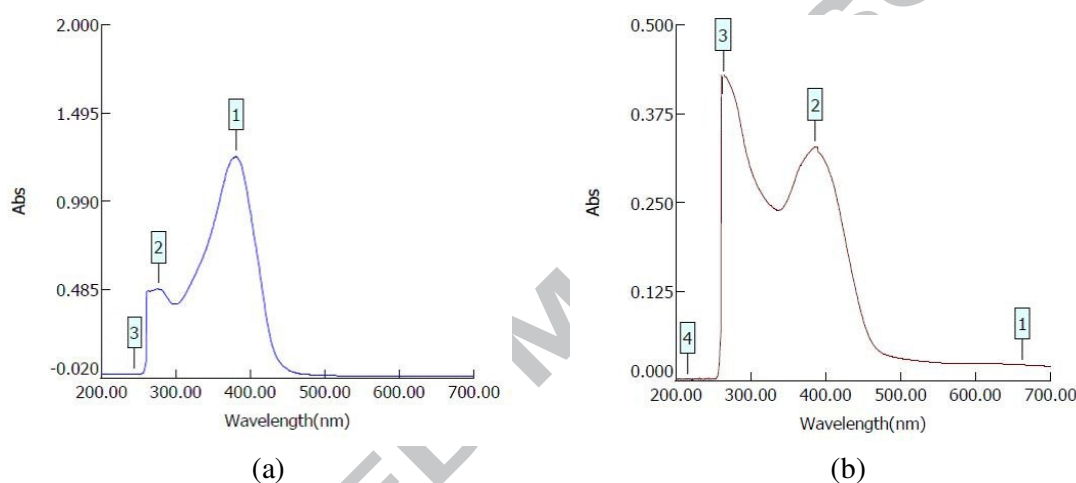


Fig. 3. Experimental UV-Visible spectra of the (a) SBHBP ligand and (b) the $[\text{Cu}_2(\text{SBHBP})_2]$ complex

3.2. Theoretical section

3.2.1. Molecular geometry and potential energy surface scan

The optimised geometry and the atom numbering scheme of the asymmetric ligand (SBHBP), under investigation is presented in Fig. 4. The ground state optimized structural parameters, such as bond length, bond angle and dihedral angle values using the B3LYP method with 6-31G(d,p) and 6-31++G(d,p) basis sets are presented in Table 2. The global minimum energy of the asymmetric ligand (SBHBP) is calculated to be about -98042.6955 eV at B3LYP/6-31++G(d,p) levels of theory. The total dipole moment of the SBHBP molecule is 2.662 Debye. DFT calculations reveal that the aldehyde rings are essentially non-planar and make

dihedral angles of 150.81 and 177.13° with the *p*-phenylenediamine ring (Fig. 4). The phenol-imine and keto-amine tautomeric forms of *N,N'*-(salicylidene)-5-bromo-2-hydroxybenzaldehyde-*p*-phenylenediamine (SBHBP) have been also optimized in gas media employing the B3LYP/6-31++G(d,p) level of theory, and the optimized tautomers are shown in Fig.5. Harmonic vibrational frequencies have been obtained at the same level of theory, and they clearly indicate that all the optimized structures of the tautomers of SBHBP are at stationary points on the potential energy surface without any imaginary frequencies. The present calculations show that among the two tautomers of SBHBP, the phenol-imine form is more stable than keto-amine form in all media. In the gas phase, the dienol form is more stable by 13.45 kcal mol⁻¹ with respect to the least stable diketo form.

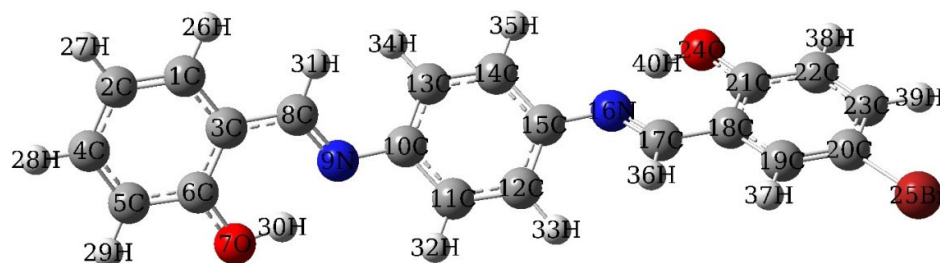


Fig. 4. Molecular structure with the atom numbering of SBHBP calculated at B3LYP/6-31++G(d,p) level.

Table 2. The calculated geometric parameters of SBHBP, bond lengths in angstrom (Å) and angles in degrees (°).

Parameters	Bond lengths (Å)		Parameters	Bond angles (°)		Parameters	Dihedral angle (°)	
	6-31++G(d,p)	6-31G(d,p)		6-31++G(d,p)	6-31G(d,p)		6-31++G(d,p)	6-31G(d,p)
C(21)-O(24)	1.342	1.337	C(14)-C(15)-N(16)	117.68	117.63	C(17)-C(18)-C(21)-O(24)	0.11	0.13
C(17)-N(16)	1.293	1.293	C(12)-C(15)-N(16)	123.59	123.68	C(23)-C(22)-C(21)-O(24)	179.93	179.90
N(16)-C(15)	1.406	1.405	C(15)-N(16)-C(17)	121.68	121.72	C(21)-C(18)-C(17)-N(16)	-0.54	-0.63
C(17)-C(18)	1.451	1.449	C(18)-C(17)-N(16)	121.87	121.87	C(11)-C(12)-C(15)-N(16)	-178.65	-
C(20)-C(19)	1.383	1.382	C(21)-C(15)-N(16)	119.27	119.24	C(15)-N(16)-C(17)-C(18)	177.29	177.34

			C(18)- C(19)			C(17)-C(18)		
C(11)- C(12)	1.390	1.388	C(14)- C(15)- C(12)	118.64	118.62	C(12)- C(15)- N(16)-C(17)	-32.33	-31.58
C(11)- C(10)	1.406	1.405	C(21)- O(24)- H(40)	107.03	107.03	C(19)- C(18)- C(17)-N(16)	179.35	179.63
C(20)- Br(25)	1.906	1.912	C(18)- C(21)- O(24)	121.89	121.99	C(15)- C(12)- C(11)-C(10)	-1.06	-0.98
O(24)-N(16)	2.627	2.620	O(24)- H(40)-N(16)	147.35	148.03	C(20)- C(19)- C(18)-C(17)	179.88	179.91
N(16).. H(40)	1.731	1.719	C(19)- C(20)-Br(25)	119.88	119.95	Br(25)- C(20)-C(19)- C(18)	-179.84	- 179.82

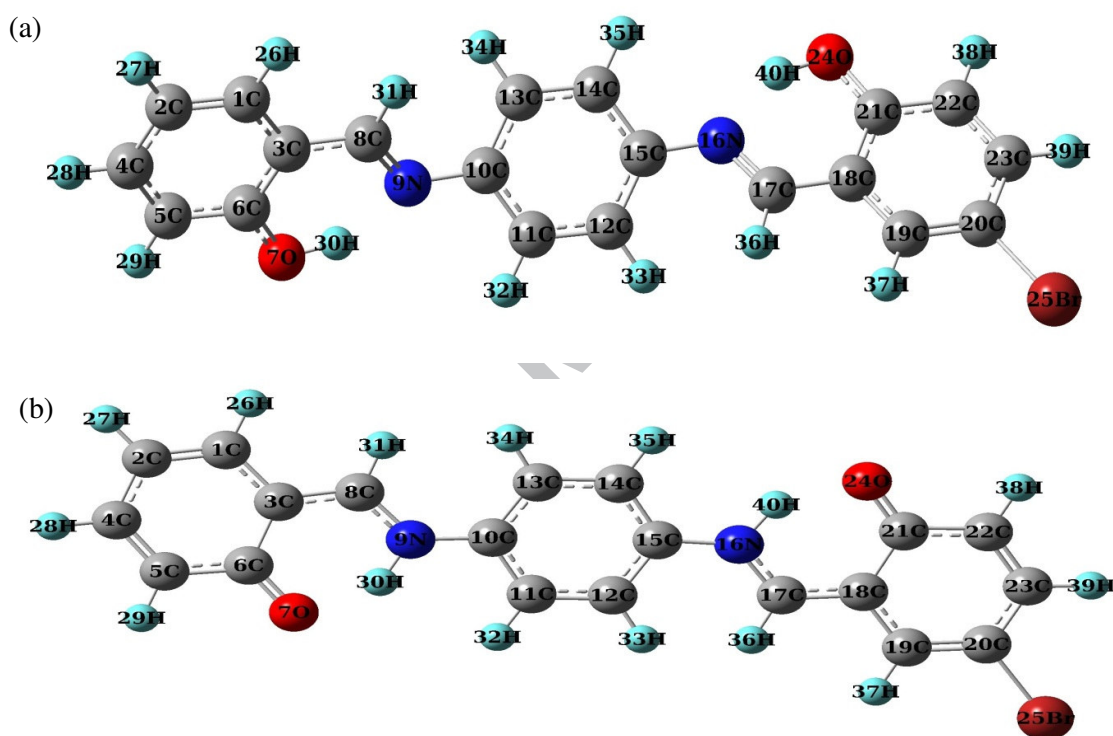


Fig. 5. The optimized geometries of (a) the phenol-imine and (b) the keto-amine tautomeric forms of SBHBP ligand at the B3LYP/6-31++G(d,p) level of theory.

In order to investigate all the possible conformations of the SBHBP ligand, a detailed potential energy surface (PES) scan for the C11–C10–N9–C8 dihedral angle was performed (Fig. 6). The scan was performed by minimizing the potential energy for all geometrical parameters by changing the dihedral angle every 30° for a 360° rotation around the bond. The shape of the potential energy as a function of the dihedral angle is given in Fig. 6. The conformational energy profile shows two maxima near the 120° and 300° dihedral angles. It is

clear from Fig. 6, there is one local minimum observed at 0° or 360° for the C₁₁–C₁₀–N₉–C₈ dihedral angles. Therefore, the most stable conformer is for the 0° and 360° dihedral angles.

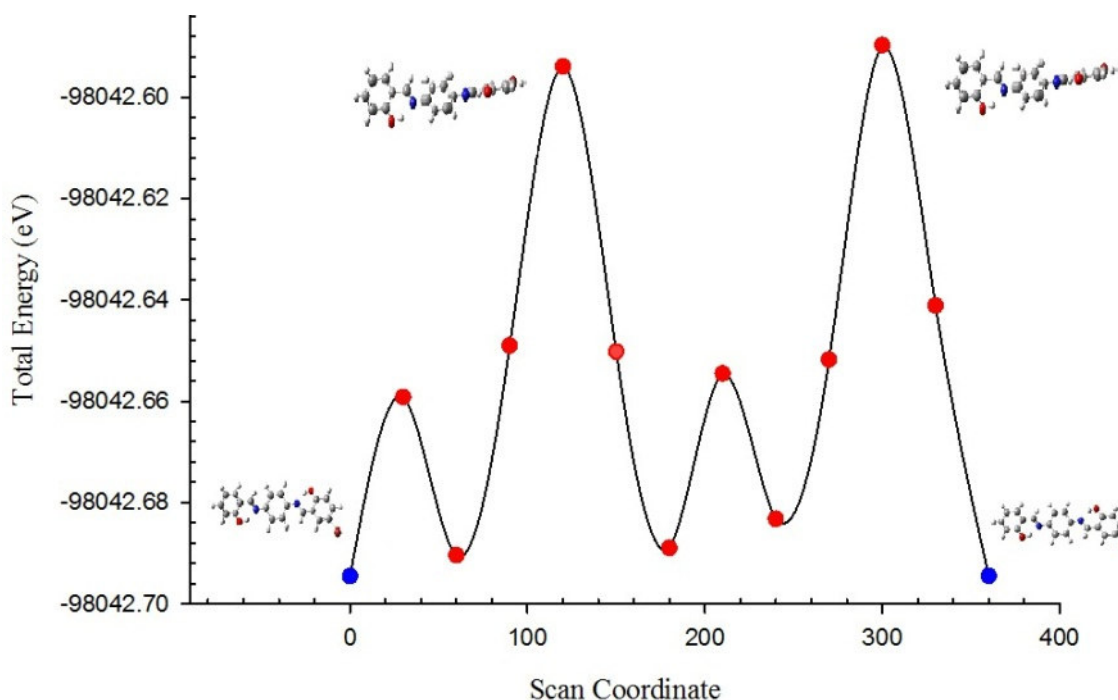


Fig. 6. Potential energy surface scan for the C₁₁–C₁₀–N₉–C₈ dihedral angle of the SBHBP ligand.

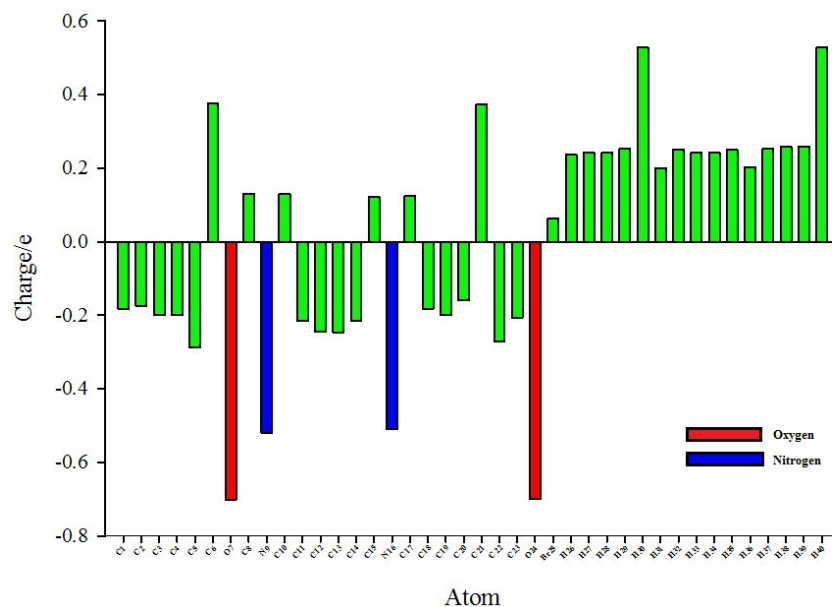
3.2.2. Atomic charges of the Schiff base ligand (SBHBP)

The NBO and Mulliken atomic charges [34] of the SBHBP ligand were also analyzed according to the results calculated at the B3LYP 6-31G(d,p) and 6-31++G(d,p) levels, and the results are listed in Table 3. The NBO charge distribution of the SBHBP ligand is determined by the B3LYP/6-31++G(d,p) method with respectable accuracy, as shown in Fig 7. Most of the carbon atoms contain negative charges and the NBO charges on the carbon atoms range from -0.122 to -0.288 atomic charge unit (a.ch.u.). The carbon atom (C₅) is the most negative carbon atom. The Mulliken and NBO charge populations show that there is a high positive charge on the hydrogen atoms (H₃₀, H₄₀), which could suggest that the reaction corresponds to a proton transfer. This is in agreement with previously reported examples in the literature that have shown that the hydrogen bonding leads to charge rearrangement [35,36]. The negativity of the oxygen atoms increases significantly in the O–H···N hydrogen

bond in comparison with the corresponding negativity in the OH group of the phenol unit. At the same time the hydrogen atoms (H₃₀, H₄₀) become more positive upon hydrogen bonding. The population of charge for the donor oxygen (O₇, O₂₄) is much larger than that of the acceptor nitrogen (N₉, N₁₆). The N₉ and N₁₆ atoms have negative NBO charges of -0.519 and -0.508 respectively, suggesting they act as possible donors to metal ions. On the other hand, the O₇ and O₂₄ atoms of the hydroxyl groups have a significant negative NBO charge (-0.701 and -0.699 a.ch.u.) and they also serve as another coordinating site to metal ions. The NBO and Mulliken atomic charges clearly indicate that the SBHBP ligand can act as a tetradentate ligand through the imine N and hydroxyl O atoms.

Table 3. Selected NBO and Mulliken charges of SBHBP at the B3LYP/6-31G(d,p) and 6-31++G(d,p) levels.

Atom	NBO		Mulliken	
	6-31++G(d,p)	6-31G(d,p)	6-31++G(d,p)	6-31G(d,p)
O ₇	-0.701	-0.691	-0.503	-0.566
O ₂₄	-0.699	-0.689	-0.505	-0.565
N ₉	-0.519	-0.521	-0.129	-0.600
N ₁₆	-0.508	-0.514	-0.130	-0.601
H ₄₀	0.528	0.520	0.505	0.354
H ₃₀	0.528	0.520	0.506	0.352
C ₆	0.376	0.390	-0.336	0.311
C ₂₁	0.373	0.386	-0.479	0.317
Br ₂₅	0.063	0.052	0.062	-0.133



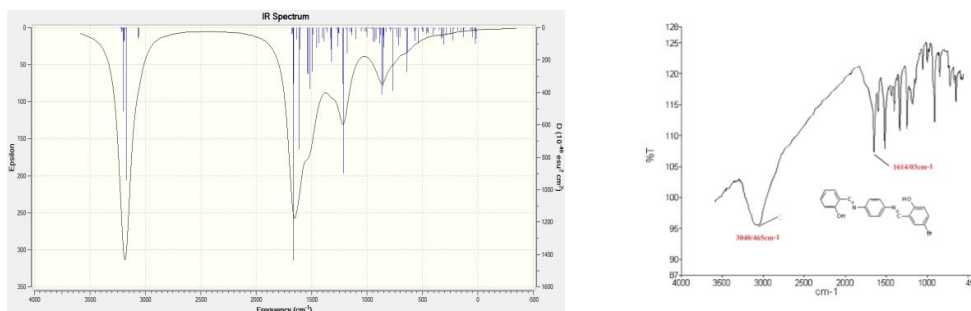


Fig. 8. Calculated, at 6-31++G(d,P) level, and experimental wavenumbers of the SBHBP ligand

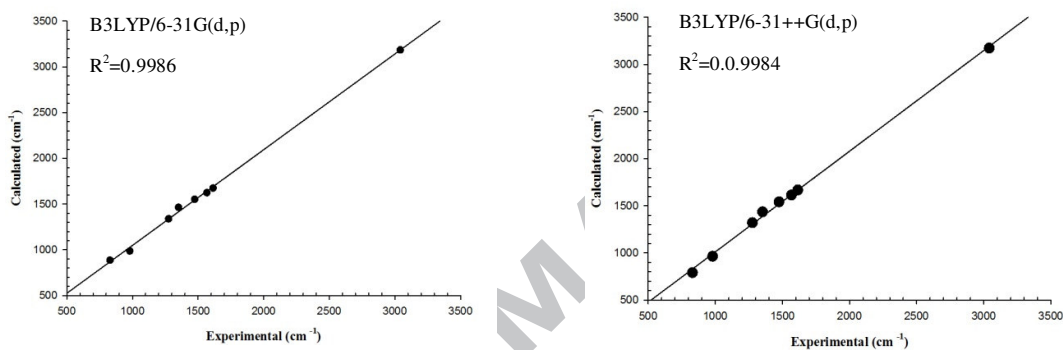


Fig. 9. Correlation graphics of calculated vs. experimental wavenumbers of the SBHBP ligand.

Table 4. Comparison of the experimental and calculated vibrational frequencies (cm^{-1}).

Experimental	Basis Set		Assignments
	6-31++G(d,p)	6-31G(d,p)	
3040.465	3173.06	3184.40	ν_s (O-H)
1614.03	1667.09	1673.73	ν_s (C=N)
1567.28	1613.35	1623.07	ν_s (O-H)
1474.19	1541.35	1550.53	ν_s (O-H)
1350.90	1435.28	1462.79	β aliphatic(HCN) + ν (NC)
1275.53	1319.82	1337.40	ν (COH) + β (HCC)
979.77	962.89	986.32	ν_s (C-H)

828.98	790.56	885.61	β R2(CCC) + β R1(CCC)
--------	--------	--------	--------------------------------------

ν , stretching; β , in-plane bending; s, symmetric; Abbreviations: R1 phenylenediamine ring; R2, aldehyde rings.

3.2.4. Solvent effects

In order to evaluate the energetic behavior of the SBHBP ligand in solvent media, we carried out calculations in five kinds of solvent with different dielectric constants ($\epsilon = 78.355$ - water; $\epsilon = 32.613$ - methanol; $\epsilon = 24.825$ - ethanol; $\epsilon = 10.125$ - dichloroethane; $\epsilon = 4.7113$ chloroform). All the geometries allowed relaxing after changing the solvents. The total energies and dipole moments were calculated in solvent media by the B3LYP method with 6-31G(d,p) and 6-31++G (d,p) levels using Onsager and PCM models, and the results are presented in Table 5. According to Table 5, it can be concluded that obtained total energies of the SBHBP ligand by Onsager and PCM decrease with increasing polarity of the solvent, and the stability of the compound increases on going from the gas phase to the solution phase [40]. The energy difference between gas phase and solvent media is given in Fig. 10, for both methods. As can be seen from Fig. 9, the PCM method (6-31++G (d,p)) provides a more stable structure than Onsager's method (5.362 kCal/mol average).

Table 5. Total energies and dipole moments of the SBHBP ligand in different solvents

Method/Solvent	ϵ^a	ΔE^b (kcal/mol)		μ (D)	
B3LYP(gas)	1			2.5721	
Onsager		6- 31++G(d,p)	6- 31G(d,p)	6- 31++G(d,p)	6- 31G(d,p)
Chloroform	4.7113	-0.3130	-0.2831	3.9061	3.7089
Dichloroethane	10.125	-0.4232	-0.3799	4.4509	4.1812
Ethanol	24.825	-0.5000	-0.4460	4.8622	4.5257
Methanol	32.613	-0.5145	-0.4583	4.9423	4.5914
Water	78.3553	-0.5431	-0.4825	5.1041	4.7232
PCM					
Chloroform	4.7113	-5.2218	-4.4659	3.1832	3.0093
Dichloroethane	10.125	-6.4690	-5.5266	3.3192	3.1125
Ethanol	24.825	-7.2028	-6.1494	3.4040	3.1743
Methanol	32.613	-7.3298	-6.2570	3.4190	3.1851

Water	78.3553	-7.5728	-6.4629	3.4483	3.2059
^a ϵ = dielectric constant, ^b $\Delta E = E_{\text{Solvation}} - E_{\text{Gas}}$					

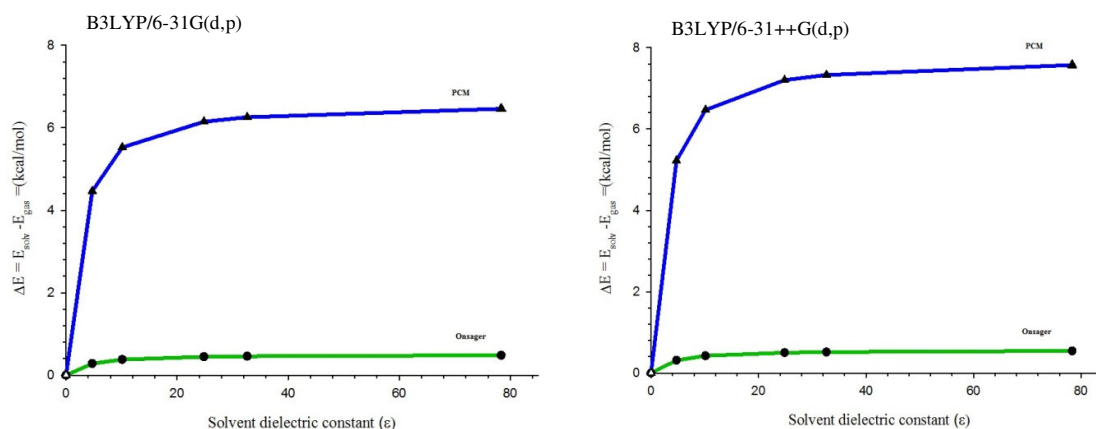


Fig. 10. Energy difference between the gas phase and solvent media by PCM and Onsager methods at the B3LYP/6-31G(d,p) and 6-31++G(d,p) levels of theory.

3.2.5. Molecular electrostatic potential and contour maps

Molecular electrostatic potential (MEP) mapped surfaces illustrate the charge distributions of molecules three dimensionally which give a clear signature of the interactions of the molecules. The electrostatic potential is used to find the reactive sites of a molecule. The molecular electrostatic potential (MEP) is related to the electronic density and is a very useful descriptor in understanding sites for electrophilic attack and nucleophilic reactions as well as hydrogen bonding interactions [41,42]. The MEP mapped surface of the molecule was calculated by the B3LYP method with the 6-31++G(d,p) basis set at 0.02 a.u. isovalues for the MO surface and 0.004 a.u. isodensity surface values. The different values of the electrostatic potential at the surface are represented by different colors. The potential increases in the order: red < orange < yellow < green < blue. The color codes of these maps are in the ranges between -1.0229 eV (deepest red) to +1.0229 eV (deepest blue) in the compound. In the color scheme of the MEP plot, the red region show atoms with lone pairs or negative electrostatic potentials; the intensity of the color is proportional to the absolute value of the potential energy. The positive electrostatic potentials are shown in the blue/yellow color region and characterize the polar hydrogen in O-H bonds. The green areas cover parts of the molecule where the electrostatic potentials are close to zero (C-C, C-N and C-Br bonds). As can be

seen from the MEP map (Fig. 11) of the SBHBP ligand, this molecule has several possible sites for electrophilic attack. The negative regions are mainly over the oxygen atoms on each of the OH groups. The negative potential surface map values are -1.0068 eV for oxygen atoms and -0.380 eV for the N atom in imine groups. However, the oxygen atoms have larger negative potential values than the nitrogen atoms. The hydrogen atoms bear the maximum region of positive charge and the most positive regions were observed around the hydrogen atoms of imine groups [43].

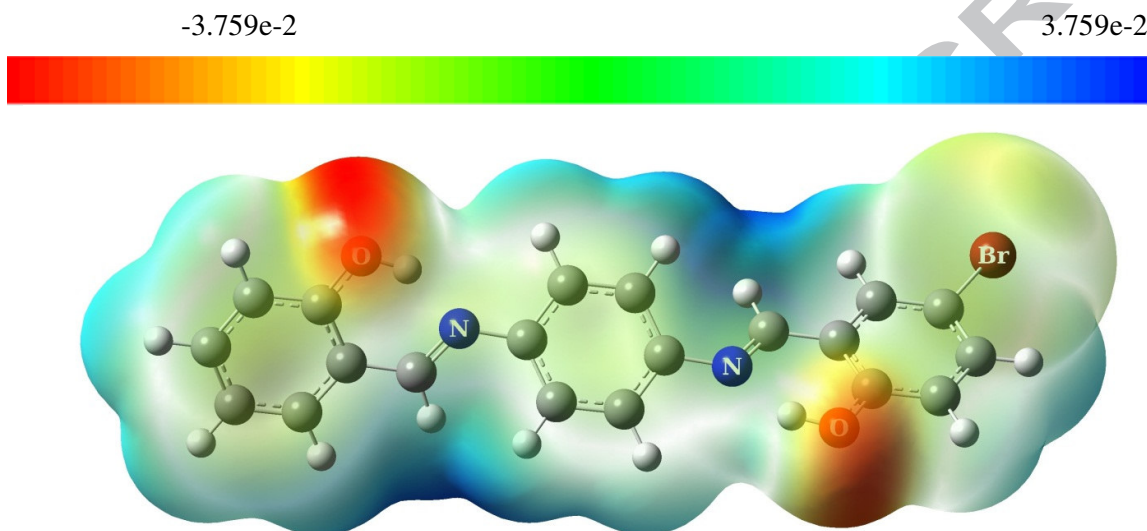


Fig. 11. Molecular electrostatic potential (MEP) map calculated at the B3LYP/6-31++G(d,p) level

3.2.6. Frontier molecular orbitals (FMOs)

The FMOs play an important role in the electric and optical properties, as well as in UV-Vis spectra and chemical reactions [44,45]. In order to evaluate the energetic behavior of the SBHBP ligand, we carried out calculations in ethanol, methanol and in the gas phase. The energies of four important molecular orbitals of SBHBP: the highest and the second highest occupied MO's (HOMO and HOMO-1), the lowest and the second lowest unoccupied MO's (LUMO and LUMO+1) were calculated using B3LYP/6-31G(d,p) and 6-31++G(d,p) and the results are presented in Table 6. The pictorial illustration of the frontier molecular orbitals and their respective positive and negative regions using B3LYP/6-31++G(d,p) are shown in Fig. 12. The positive and negative phases are represented in red and green colours,

respectively. As seen in Fig. 12, the HOMO is mainly localized on the ring carbon atoms and the bromine atom and the lowest-lying unoccupied molecular orbital (LUMO) is localized mainly over the entire molecule. While the HOMO-1 is localized on the Br atom and the LUMO+1 is localized over the whole structure. The values of the energy separation between the HOMO and LUMO are 3.5539, 3.5531 and 3.4929 eV in methanol, ethanol and gas phase, respectively [45]. The HOMO→LUMO transition implies that an intramolecular charge transfer takes place within the molecule [46]. The energy gap (E_g) of SBHBP has been calculated from the HOMO and LUMO levels. Molecules with a large energy gap are chemically stable molecules. Hard molecules have a large energy gap and they are more stable than soft molecules having a small energy gap. Since soft molecules have a small energy gap, they are more polarizable and more reactive than hard molecules. The value of the energy separation between the HOMO and LUMO for SBHBP ligand is 3.4929eV (in the gas phase) and this low energy gap indicates that the thermodynamics of the SBHBP structure are not stable. The HOMO-LUMO energy separation has been used as a simple indicator of kinetic stability [47]. The higher the energy of the HOMO, the easier it is for the HOMO to donate electrons, whereas it is easier for the LUMO to accept electrons when the energy of the LUMO is low. The dipole moment in a molecule is an important electronic property which results from a non-uniform distribution of charges on the various atoms in a molecule. Based on the predicted dipole moment values, it was found that in going to the solvent phase from the gas phase, the dipole moment value increases (Table 6).

Table 6. Calculated energies and Dipole moment values of the SBHBP ligand in methanol, ethanol and in the gas phase.

B3LYP	Methanol		Ethanol		Gas	
	6-	6-	6-	6-31	6-	6-
$E_{\text{total}}(\text{eV})$	-	-	-	-	-	-
$E_{\text{HOMO}}(\text{eV})$	-5.7526	-6.0291	-5.7520	-6.0291	-5.8914	-6.0729
$E_{\text{LUMO}}(\text{eV})$	-2.1932	-2.4752	-2.1932	-2.4760	-2.2580	-2.5800
$\Delta E_{\text{HOMO-LUMO}}$	3.5594	3.5539	3.5588	3.5531	3.6334	3.4929
$E_{\text{HOMO-1}}(\text{eV})$	-6.1632	-6.4607	-6.1616	-6.4593	-6.1007	-6.4258
$E_{\text{LUMO+1}}(\text{eV})$	-1.5279	-1.8316	-1.5279	-1.8322	-1.5764	-1.9184
$\Delta E_{\text{HOMO-1-LUMO+1}}$	4.6353	4.6291	4.6337	4.6271	4.5243	4.5074
Dipole moment (μ)	3.1851	3.4190	3.1743	3.4040	2.5721	2.6628

33

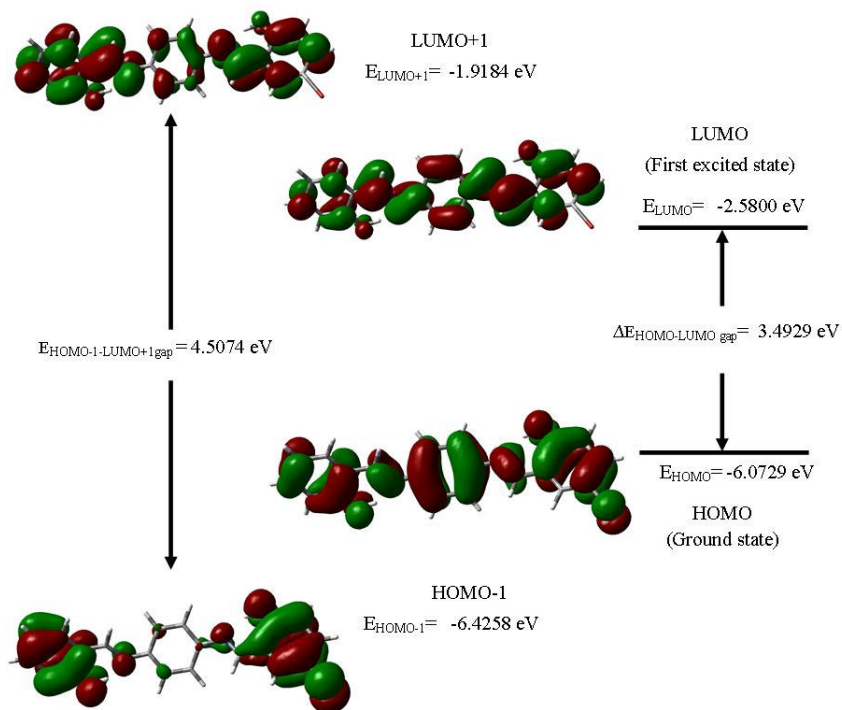


Fig. 12. Molecular orbital surfaces and energy levels given in parentheses for the HOMO–1, HOMO, LUMO and LUMO+1 of the SBHBP ligand in the gas phase computed at the B3LYP/6-31++G(d,p) level

3.2.7. Ultraviolet spectra analysis

The ultraviolet spectra of the SBHBP ligand have been investigated in the methanol, ethanol and gas phase by theoretical calculations. On the basis of the fully optimized ground-state structure, the time-dependent DFT (TD-DFT) method at the B3LYP6-31G(d,p) and 6-31++G(d,p) levels of theory have been used to determine the low-lying excited states of the SBHBP ligand. The theoretical electronic excitation energies, absorption wavelength and oscillator strengths are listed in Table 7. Calculations of the molecular orbital geometry show that the maximum absorption wavelength corresponds to the electronic transition from the HOMO \rightarrow LUMO, and other electronic transitions with a smaller contribution correspond to the HOMO – 1 \rightarrow LUMO and HOMO - 2 \rightarrow LUMO transitions. The observed transition from the HOMO \rightarrow LUMO is $n \rightarrow \pi^*$.

The calculated absorption maxima values were found using the B3LYP/6-31++G(d,p) method as 401.56, 362.16, 338.51 nm for gas phase, 402.78, 350.72, 333.00 nm for methanol

solution and 403.54, 351.06, 333.23 nm for ethanol solution. As can be seen, the calculations performed for methanol and ethanol are very close to each other when compared with the gas phase. Also it can be observed that the calculated peaks in the gas phase are in good agreement with the experimental peaks, Fig. 13.

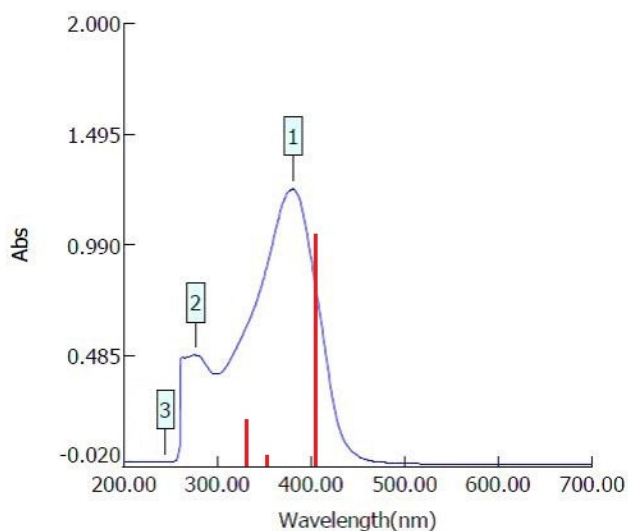


Fig.13. Experimental and calculated UV-Visible spectra of the SBHBP ligand at the 6-31++G(d,p) level in the gas phase

Table 7. Experimental and calculated absorption wavelengths (λ), excitation energies (E) and oscillator strengths (f) of the SBHBP ligand in methanol, ethanol and in the gas phase.

TD- B3LYP/6-31G(d,p)												
Experimental		Gas			Methanol			Ethanol			Gas	
(nm) λ	E (eV)	E (eV)	(nm) λ	(f)	E (eV)	(nm) λ	(f)	E (eV)	(nm) λ	(f)	Assignment	Major contribution ^a
											State	Percentage (%)
381	3.254	3.111	398.4	1.061	3.098	400.1	1.292	3.093	400.8	1.301	Single t	$n \rightarrow \pi^*$ H \rightarrow L (98%)
	5	5	7		9	0		1	4			
277	4.476	3.432	361.1	0.013	3.534	350.8	0.008	3.530	351.1	0.009	Single t	$\pi \rightarrow \pi^*$ H-1 \rightarrow L (96%)
	5	6	9		1	2		9	4			
244	5.081	3.700	335.0	0.227	3.744	331.0	0.131	3.742	331.3	0.132	Single t	$n \rightarrow \pi^*$ H-2 \rightarrow L (93%)
	9	7	3		8	8		4	0			
TD- B3LYP/6-31++G(d,p)												
Experimental		Gas			Methanol			Ethanol			Gas	
(nm) λ	E (eV)	E (eV)	(nm) λ	(f)	E (eV)	(nm) λ	(f)	E (eV)	(nm) λ	(f)	Assignment	Major contribution ^a
											State	Percentage (%)
381	3.254	3.087	401.5	1.077	3.078	402.7	1.312	3.072	403.5	1.321	Single t	$n \rightarrow \pi^*$ H \rightarrow L (98%)
	5	6	6		2	8		4	4			
277	4.476	3.423	362.1	0.023	3.535	350.7	0.016	3.531	351.0	0.016	Single t	$\pi \rightarrow \pi^*$ H-1 \rightarrow L (96%)
	5	5	6		1	2		7	6			

244	5.081	3.662	338.5	0.185	3.723	333.0	0.097	3.720	333.2	0.097	Single t	n→π*	H-2 → L (93%)
	9	6	1		3	0		6	3				

^a H: HOMO; L: LUMO.

3.2.8. NMR analysis

For a comparison between experimental and theoretical NMR data, which may be helpful in making correct assignments and understanding the relationship between the chemical shift and molecular structure, ¹H NMR chemical shifts calculations for further clarification of the synthesized Schiff base ligand are reported. The "gauge independent atomic orbital" (GIAO) method [41] has proven to be quite accepted and accurate. Density functional theory (DFT) shielding calculations are rapid and applicable to large systems. To provide an explicit assignment and analysis of the ¹H NMR spectrum, theoretical calculations on the chemical shifts of the SBHBP ligand were carried out with the GIAO method at the B3LYP 6-31G(d,p) and 6-31++G(d,p) levels. The ¹H NMR theoretical and experimental chemical shifts, isotropic shielding constants and the NMR spectral assignments are presented in Table 8. To clarify the relation between the theoretical and experimental values of the NMR chemical shift constants, the experimental data were plotted versus the computed values. As can be seen, the results obtained by the theoretical are in reasonable agreement with the experimental values, with only slight differences. As shown in Fig. 14, there are good linear relationships between the experimental and theoretical B3LYP 6-31G(d,p) and 6-31++G(d,p) chemical shifts.

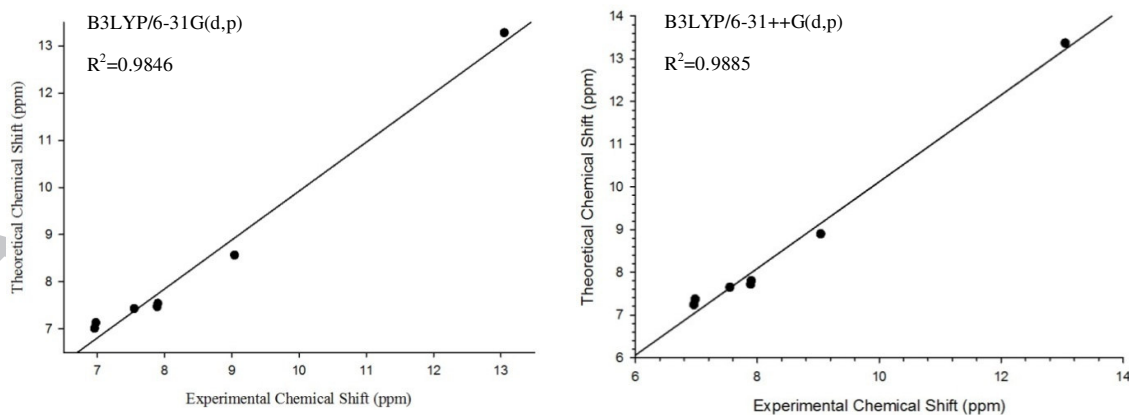


Fig. 14. Theoretical vs. experimental ¹H NMR chemical shifts of the SBHBP Schiff base.

Table 8. The experimental and theoretical ^1H isotropic chemical shifts (ppm) with respect to TMS for the SBHBP ligand

^1H Assignment	Theoretical δ (ppm)		Experimental δ (ppm)
	6-31++G(d,p)	6-31G(d,p)	
H40, H30	13.37	13.28	13.05
H36, H31	8.90	8.56	9.04
H39, H28	7.80	7.54	7.90
H35, H32	7.72	7.47	7.89
H34, H33	7.65	7.43	7.55
H37, H29	7.37	7.13	6.98
H38, H27	7.24	7.01	6.96

4. Conclusion

In this study, some experimental investigations and theoretical results were used to clarify the identification of a novel tetradentate asymmetrical Schiff base ligand and its Cu(II) binuclear complex. The ligand structural parameters, IR wavenumbers and activities of vibrational bands were calculated with the B3LYP method and 6-31G(d,p) basis set. The applied method is in good accordance with the experimental values. Quantum chemical descriptors, such as E_{HOMO} , E_{LUMO} , the energy gap between E_{HOMO} and E_{LUMO} , dipole moments, NBO and Mulliken atomic charges, ^1H NMR spectrum and molecular electrostatic potential were calculated. The value of the energy gap between the HOMO and LUMO and the chemical hardness of the ligand also increase with increasing solvent polarity. The MEP map shows that the negative potential sites are on electronegative atoms (N and O atoms) while the positive potential sites are around the hydrogen atoms. These sites give information about the region from where the compound can undergo non-covalent interactions. Natural bond orbital analysis indicates strong intramolecular interactions and are in agreement with the experimental intramolecular hydrogen bonding results. Any differences observed between the experimental and the calculated wavenumbers could be due to the fact that the calculations have been performed for a single molecule in the gaseous state, contrary to the experimental values recorded in the presence of intermolecular interactions. We hope the results of this study will help researchers in the design and synthesis new asymmetric ligands.

References

- [1] R.H. Lozier, R.A. Bogomolni, W. Stoeckenius, *Biophys. J.* 15 (1975) 955.
- [2] E.M. Hodnett, W.J. Dunn, *J. Med. Chem.* 13 (1970) 768.
- [3] M. Calligaris, L. Randaccio, *Comprehensive Coordination Chemistry*, vol. 2, Pergamon Press, London, 1987, pp. 715.
- [4] A.D. Garnovski, A.L. Nivorozhkin, V.I. Minkin, *Coord. Chem. Rev.* 126 (1993) 1.
- [5] C.A. McAuliffe, R.V. Parish, S.M. Abu-El-Wafa, R.M. Issa, *Inorg. Chim. Acta* 115 (1986) 91.
- [6] A. Prakash, D. Adhikari, *Chem. Tech. Res.* 3 (2011) 1891.
- [7] S. Zolezzi, E. Spodine, A. Decinti, *Polyhedron* 21 (2002) 55.
- [8] V. Ambike, S. Adsule, F. Ahmed, Z. Wang, Z. Afrasiabi, E. Sinn, F. Sarkar, S. Padhye, *J. Inorg. Biochem.* 101 (2007) 1517.
- [9] T. Rosu, E. Pahontu, C. Maxim, R. Georgescu, N. Stanica, G. L. Almajan, A. Gulea, *Polyhedron* 29 (2010) 757.
- [10] J. Rahchamani, M. Behzad, A. Bezaatpour, V. Jahed, G. Dutkiewicz, M. Kubicki, M. Salehi, *Polyhedron* 30 (2011) 2611.
- [11] T.W. Hambley, L.F. Lindoy, J.R. Reimers, P. Turner, W. Wei, A.N.W. Cooper, *J. Chem. Soc., Dalton Trans.* (2001) 614.
- [12] S. Chandra, L.K. Gupta, *Trans. Met. Chem.* 30 (2005) 630.
- [13] A.R. Fakhari, A.R. Khorrami, H. Naeimi, *Talanta* 66 (2005) 813.
- [14] J. Liu, B. Wu, B. Zhang, Y. Liu, *Turk. J. Chem.*, 30 (2006) 41.
- [15] I. Cianga, M. Ivanoiu, *Eur. Polym. J.* 42 (2006) 1922.
- [16] M. Dolaz, M. Tümer, M. Diğrak, *Trans. Met. Chem.* 29 (2004) 528.
- [17] H. Eshtiagh-Hosseini, M.R. Housaindokht, S.A. Beyramabadi, S. Beheshti, A.A. Esmaeili, M. Javan-Khoshkholgh, A. Morsali, *Spectrochim. Acta A* 71 (2008) 1341.

- [18] H. Eshtiagh-Hosseini, M.R. Housaindokht, S.A. Beyramabadi, S.H. MirTabatabaei, A.A. Esmaeili, M. JavanKhoshkholgh, *Spectrochim. Acta A* 78 (2011) 1046.
- [19] H. Eshtiagh-Hosseini, H. Aghabozorg, M. Mirzaei, S.A. Beyramabadi, H. Eshghi, A. Morsali, A. Shokrollahi, R. Aghaei, *Spectrochim. Acta A* 78 (2011) 1392.
- [20] A.D. Becke, *J. Chem. Phys.* 98 (1993) 5648.
- [21] C. Lee, W. Yang, R.G. Parr, *Phys. Rev. B* 37 (1988) 785.
- [22] M.J. Frisch, G.W. Trucks, H.B. Schlegel, G.E. Scuseria, M.A. Robb, J.R. Cheeseman, G. Scalmani, V. Barone, B. Mennucci, G.A. Petersson, H. Nakatsuji, M. Caricato, X. Li, H.P. Hratchian, A.F. Izmaylov, J. Bloino, G. Zheng, J.L. Sonnenberg, M. Hada, M. Ehara, K. Toyota, R. Fukuda, J. Hasegawa, M. Ishida, T. Nakajima, Y. Honda, O. Kitao, H. Nakai, T. Vreven, J.A. Montgomery Jr., J.E. Peralta, F. Ogliaro, M. Bearpark, J.J. Heyd, E. Brothers, K.N. Kudin, V.N. Staroverov, R. Kobayashi, J. Normand, K. Raghavachari, A. Rendell, J.C. Burant, S.S. Iyengar, J. Tomasi, M. Cossi, N. Rega, J.M. Millam, M. Klene, J.E. Knox, J.B. Cross, V. Bakken, C. Adamo, J. Jaramillo, R. Gomperts, R.E. Stratmann, O. Yazyev, A.J. Austin, R. Cammi, C. Pomelli, J.W. Ochterski, R.L. Martin, K. Morokuma, V.G. Zakrzewski, G.A. Voth, P. Salvador, J.J. Dannenberg, S. Dapprich, A.D. Daniels, O. Farkas, J.B. Foresman, J.V. Ortiz, J. Cioslowski, D.J. Fox, *Gaussian 09, Revision A. 02*, Gaussian, Inc., Wallingford, CT, 2009.
- [23] R. Dennington II, T. Keith, J. Millam, *GaussView, Version 4.1.2*, Semichem, Inc., Shawnee Mission, KS, 2007.
- [24] K. Wolinski, J.F. Hilton, P. Pulay, *J. Am. Chem. Soc.* 112 (1990) 8251.
- [25] J.L. Dodds, R. McWeeny, A.J. Sadlej, *Mol. Phys.* 41 (1980) 1419.
- [26] L. Onsager, *J. Am. Chem. Soc.* 58 (1936) 1486.
- [27] J. Tomasi, B. Mennucci, R. Cammi, *Chem. Rev.* 105 (2005) 2999.
- [28] D.C. Young, *Computational Chemistry: A Practical Guide for Applying Techniques to Real World Problems (Electronic)*, John Wiley & Sons Inc., New York, 2001, p.267.
- [29] H. Nazır, M. Yıldız, H. Yılmaz, M.N. Tahir, D. Ülkü, *J. Mol. Struct.* 524 (2000)241.

- [30] K. Nakamoto, *Infrared and Raman Spectra of Inorganic and Coordination Compounds*, John Wiley & Sons Inc., New York, 1978, p.339.
- [31] W. Kemp, *Organic Spectroscopy*, John Wiley & Sons Inc., New York, 1975, p. 248.
- [32] B.S. Creaven, M. Devereux, A. Foltyn, S. Mcclean, G. Rosair, V. R. Thangella, M. Walsh, *Polyhedron* 29 (2010) 813.
- [33] D. Nartop, P. Gurkan, N. Sari, S. Cete, *J. Coordination. Chem.* 61 (2008) 3516.
- [34] A.E. Reed, R.B. Weinstock, F. Weinhold, *J. Chem. Phys.* 83 (1985) 735.
- [35] Y. Dimitrova, *Spectrochim. Acta A* 69 (2008) 517.
- [36] S. Sebastian, S. Sylvestre, D. Jayarajan, M. Amalanathan, K. Oudayakumar, T. Gnanapoongothai, T. Jayavarthanam, *Spectrochim. Acta A* 101 (2013) 370.
- [37] A.D. Becke, *J. Chem. Phys.* 98 (1993) 5648-5652.
- [38] H. Tanak, *Comput. Theor. Chem.* 967 (2011) 93.
- [39] K. Balci, S. Akyuz, *Vib. Spectrosc.* 48 (2008) 215.
- [40] Y.B. Alpaslan, G. Alpaslan, A.A. Agar, N.O. Iskeleli, E. Oztekin, *J. Mol. Struct.* 995 (2011)58.
- [41] F.J. Luque, J.M. Lopez, M. Orozco, *Theor. Chem. Acc.* 103 (2000) 343.
- [42] T.U. Devi, S. Priya, S. Selvanayagam, K. Ravikumar, K. Anita, *Spectrochim. Acta A* 97 (2012) 1063.
- [43] M. Karabacak, E. Kose, A. Atac, *Spectrochim. Acta A* 91 (2012) 83.
- [44] I. Fleming, *Molecular Orbitals and Organic Chemical Reactions: Student Edition*, John Wiley & Sons, Ltd, Chichester, 2009, p. 61.
- [45] U. Rani, M. Karabacak, O. Tanriverdi, M. Kurt, N. Sundaraganesan, *Spectrochim. Acta A* 92 (2012) 67.
- [46] R.G. Pearson, *Proc. Natl. Acad. Sci.* 83 (1986) 8440.
- [47] K.H. Kim, Y.K. Han, J. Jung, *Theor. Chem. Acc.* 113 (2005) 233.

Graphical Abstract:

A new asymmetrical Schiff base ligand (SBHBP) and its binuclear Cu(II) complex have been synthesized. The molecular structures and spectroscopic properties of the ligand and its complex were experimentally characterized by spectroscopic techniques and computationally by the density functional theory (DFT) method. A potential surface scan study was carried out and the most stable geometry of the SBHBP ligand was confirmed. The theoretical vibrational frequencies are in good agreement with the experimental values. Additionally, Mulliken and NBO atomic charges, NMR analysis, molecular electrostatic potential (MEP) and frontier molecular orbitals (FMO) analysis of the SBHBP ligand were also investigated using theoretical calculations.

